Divergence of Iron and Manganese Oxidation State Distributions, Bonding Environments, and Mobility in Mining-impacted Lake Sediments: Column Experiments

A Thesis

Presented in Partial Fulfillment of the Requirements for

the Degree of Master of Science with a

Major in Water Resources

in the

College of Graduate Studies

University of Idaho

by

Gaige Swanson

Approved by:

Major Professor: Jeff B. Langman, Ph.D.

Committee Members: Frank M. Wilhelm, Ph.D.; James Moberly, Ph.D.

Department Administrator: Timothy Link, Ph.D.

August 2022

Abstract

The mobility of a metal in mining-impacted sediments is determined by the environmental conditions that influence the metal's oxidation state and bonding environment. Coeur d'Alene Lake of northern Idaho, USA, has been impacted by legacy mining practices that allowed the hydrologic transport of mining waste to the lakebed, which resulted in the deposition of an estimated 75 Mt of metal(loid)-rich sediments containing As, Cd, Fe, Mn, Pb, and Zn over the past 100+ years. Future lake conditions may include substantial algal blooms and deposition of additional algal detritus to the sediment-water interface, which may alter metal remobilization/retention during seasonal anoxia. Cores of the lake sediments were exposed to anoxic and anoxic + algae conditions for eight weeks. Over the eight-week period and at a location 12.5 cm deep in the sediments, anoxic and anoxic + algae conditions produced relatively stable Fe and Mn oxidation states and bonding environments. At a location 2.5 cm below the sediment-water interface, anoxic conditions promoted a relatively stable environment in which Fe and Mn oxidation states did not vary greatly during the experiment. At the 2.5-cm depth, the anoxic + algae condition substantially altered the Mn oxidation state distribution and bonding environment, but this condition did not strongly influence the Fe oxidation state distribution or bonding environment. The addition of algal detritus increased the presence of Mn^{3+}, at select times produced Mn^{4+}, altered the Mn bonding environment, and induced a larger release of Mn from the sediments into porewater. This increased oxidation of Mn, change in Mn bonding environment, and additional release of Mn from the sediments under the anoxic + algae condition likely occurred because of the increased formation of organo-Mn complexes produced during enhanced enzymatic processes with the presence of the additional organic matter. The increased microbial activity and Mn mobility has the potential to increase the release of Mn from the sediments and into the lake water column.

Acknowledgments

I would like to acknowledge the following faculty for shaping my academic career into a pursuit of knowledge and understanding of water as it relates to the environment:

Jeff B. Langman, Ph.D., for teaching me the fundamentals of hydrogeology and providing hands on experience with numerous projects and courses throughout my academic career and taking me on as his graduate student.

Matthew J. Morra, Ph.D., for creating the spark that got me interested in chemical fate and transport that steered my interests into the realm of water quality, as well as convincing me to further my knowledge and pursue an M.S. in Water Resources.

Jerry P. Fairley, Ph.D., for giving me valuable industry knowledge and experience in hydrology which provided me hands on experience in the realm of water quantity.

And to my committee, Frank M. Wilhelm, Ph.D.; James Moberly, Ph.D., for providing me feedback and support.

Table of Contents

Title Page i

Abstract ii

Acknowledgments iii

Table of Contents iv

List of Figures v

Chapter 1: Introduction 1

Environmental change and manganese cycling 2

Chapter 2: Study area, Materials, and Methods 4

Study design 4

Sediment core collection 5

Algae collection and column loading 5

Column experiment 5

X-ray absorption spectroscopy 6

Chaper 3: Results 9

Reactive upper sediment layer 9

Iron and manganese oxidation state distribution 10

Upper sediment iron and manganese bond environment 12

Chapter 4: Discussion 16

Chaper 5: Conclusion 19

References 20

List of Figures

Figure 1. Coeur d'Alene Lake, River, and Mining District (Silver Valley) in northern Idaho, USA

Figure 2. Cumulative area graphs of major (a) and trace element (b) concentrations for sediments collected from Aberdeen Lodge Bay in Coeur d'Alene Lake. Major elements are normalized to 100 percent. Trace element concentrations are not normalized (Langman et al., 2020a).

Figure 3. Iron and manganese concentrations in porewater extracted from the control (anoxia) and treatment (anoxia + algae) cores over the course of the 8-week experiment (Langman et al., 2020a). Iron (2+) concentration in upper sediments porewater indicated by dashed line.

Figure 4. Distribution of iron oxidation states in upper and lower sediment samples of the control (anoxia) and treatment (anoxia + algae) cores over the course of the 8-week experiment.

Figure 5. Distribution of manganese oxidation states in upper and lower sediment samples of the control (anoxia) and treatment (anoxia + algae) cores over the course of the 8-week experiment.

Figure 6. Fourier transformation of iron EXAFS spectra (magnitude ($\chi(R)$) and real portion ($Re[(\chi(R)])$) for upper sediments from the anoxia and anoxia + algae cores over the course of the 8-week experiment.

Figure 7. Fourier transformation of manganese EXAFS spectra (magnitude ($\chi(R)$ and real portion $Re[(\chi(R)])$) for upper sediments from the anoxia and anoxia + algae cores over the course of the 8-week experiment.

Figure 8. Schematic of possible enzymatic manganese cycling in the presence of detrital organic matter. The green arrow represents a potential pathway that occurs by means of an oxidase that forms mobile Mn^{4+} (adapted from Hofrichter (2002).

Chapter 1: Introduction

The impact of legacy mines is a global issue that has resulted in extensive metal contamination of natural environments, such as the substantial contamination of Coeur d'Alene Lake (Harrington et al., 1998b; Horowitz et al., 1995a; National Research Council, 2005) in northern Idaho, USA (Fig. 1). Remobilization of sediment-bound metals may occur through physical (e.g., current flow) and biochemical (e.g., reduction-oxidation (redox)) processes, particularly during strong seasonal changes in environmental conditions (Ciszewski and Grygar, 2016; Gozzard et al., 2011; Huettel et al., 2003; Krantzberg, 1985; Schulz-Zunkel and Krueger, 2009). In lacustrine sediments, biochemical processes can be the primary remobilization/retention pathway given limited sediment resuspension (Hamilton-Taylor et al., 1996; Morfett et al., 1988; Palmer et al., 2019). In such instances, the seasonal alteration of the lacustrine environment with changes in temperature, redox, organic carbon, and microbial populations can induce or restrict metal mobility in lakebed sediments (Gadd, 2004; Langman et al., 2020b; Martin and Pedersen, 2002; Ni et al., 2016; Sarmiento et al., 2012; Smith and Huyck, 1999; Wang et al., 2003). An additional influence on metal mobility in mining-impacted lacustrine environments is the alteration of redox-sensitive metals, such as iron [Fe] and manganese [Mn] (Violante et al., 2010). Changes in Fe and Mn oxidation states and bonding environments can provide sorbing surfaces that allow for retention of other metals and/or produce soluble species/particles that allow transport across the sediment-water interface (SWI) and degrade water quality of the overlying water (Davison, 1993; Wang et al., 2003).

Redox-sensitive Fe has been identified as a control on the mobility of mining-related metals in Coeur d'Alene Lake sediments (Arora et al., 2015; Langman et al., 2020b; Toevs et al., 2008). Seasonal variations in the lake environment (e.g., temperature, redox) induce cycling of Fe and other metals, such as the substantial concentrations of Mn, between soluble and insoluble phases (Bostick et al., 2001; Harrington et al., 1998b; Haus et al., 2008; Langman et al., 2020b, 2020a; Morra et al., 2015). Harrington et al. (1998b) hypothesized retention of Fe and Mn in the lake sediments under reducing conditions because of metal-sulfide formation and binding of the metals with organic matter. Yet, Harrington et al. (1998b) also described mobilization of arsenic [As], Fe, and Mn and their movement towards the SWI. Langman et al. (2020a) evaluated changes in sulfur [S] oxidation states and bonding environments in Coeur d'Alene Lake sediments that were exposed to anoxic and anoxic + algae conditions over an 8-week period. The anoxic + algae condition inhibited S reduction and enhanced the release of Mn but not the release of Fe. This subsequent study examined the sediments

of (Langman et al., 2020a) for changes in Fe and Mn oxidation states and bonding environments over the course of the 8-week experiment. The goal was to understand the remobilization effect of the additional organic matter (algal detritus) on Mn but not on Fe.

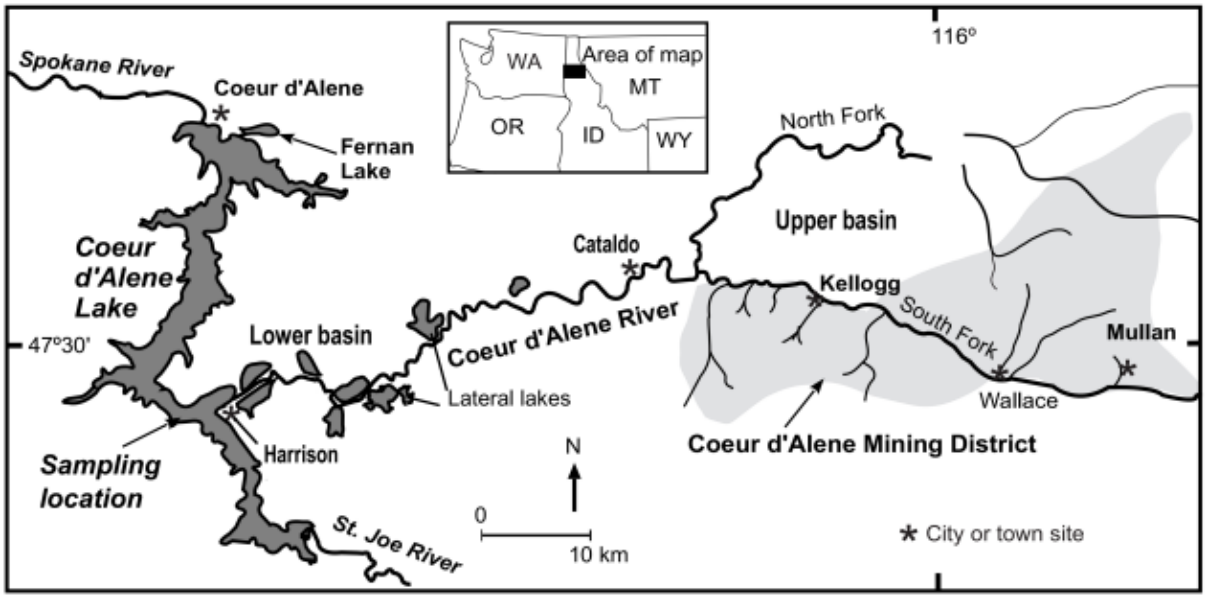

Fig. 1. Coeur d'Alene Lake, River, and Mining District (Silver Valley) in northern Idaho, USA.

1.1 *Environmental change and manganese cycling*

Legacy mining practices in the Coeur d'Alene Mining District (Fig. 1) led to the the hydrologic transport of tailings and waste rock in the Coeur d'Alene River system that resulted in the deposition of 75 Mt of metal(loid)-rich sediments in Coeur d'Alene Lake over the past 100+ years (Balistrieri et al., 1998; Horowitz et al., 1995a, 1995b; Paulson, 2001). The lake undergoes seasonal thermal stratification (thermocline formation), formation of hypoxic and anoxic water in the hypolimnion (La Force et al., 2000; U.S. Environmental Protection Agency 2020; Wood and Beckwith, 2008), and changes in redox conditions at the SWI (Arora et al., 2015; Cummings et al., 2000). Seasonal changes at the SWI can remobilize metals—such as the 470,000 t of lead [Pb] and substantial masses of silver [Ag], As, cadmium [Cd], copper [Cu], Fe, mercury [Hg], Mn, antimony [Sb], and zinc [Zn] present in lake sediments (Aiken et al., 2011; Haus et al., 2008; Kretzschmar and Schäfer, 2005; Langman et al., 2020a, 2018; Plathe et al., 2013).

The continued river input and resuspension of Zn in Coeur d'Alene Lake likely has suppressed additional algal growth (Clark and Mebane, 2014; Kuwabara et al., 2007; Morra et al., 2015; Woods and Beckwith, 1997). Historically, seasonal conditions at the lake's SWI have resulted in limited remobilization of metals (Arora et al., 2015; Harrington et al., 1998a, 1998b; Horowitz et al., 1995a, 1995b; Pedersen, 1996; Şengör et al., 2007). Yet, there is a growing concern of increased metal

remobilization because of an expected decrease in Zn inputs from upstream remediation and continued phosphorus loading (Aiken et al., 2011; Balistrieri et al., 2003; Balistrieri and Blank, 2008; Gao et al., 2003; Hoffmann et al., 2007). With a decrease in Zn, future conditions may produce algal blooms similar to eutrophic and mesotrophic lakes in the region (Child et al., 2018), which likely will increase algae growth and deposition of additional organic matter to the lakebed (Farley, 2012). Given the enhanced release of Mn, but not an enhanced release of Fe, with the addition of algal detritus to the lake sediments (Langman et al., 2020a), this study was implemented to evaluate changes in Mn and Fe oxidation states and bonding environments that can indicate influences on Mn mobility. An availability of Mn along with the usual presence of Fe (Boyle, 2001; Davison, 1993) in these lacustrine sediments allows these metals to participate in a variety of biogeochemical processes, which may include humic acid degradation (Stone and Morgan, 1984; Sunda and Kieber, 1994), trace element cycling (Murray and Tebo, 2007; Nelson et al., 1999), and the coupled processes of carbon oxidation and anaerobic respiration (Nealson and Saffarini, 1994). The transformation of Fe and Mn in an anoxic sediment environment occurs through abiotic and microbially-catalyzed (e.g., bacteria, fungi, cyanobacterium, algal phototrophs) reactions that lead to the formation of Fe/Mn minerals and organometallic compounds that may or may not be soluble (Andeer et al., 2015; Bargar et al., 2005; Brouwers et al., 1999; Butterfield et al., 2013; Melton et al., 2014; Qin et al., 2017; Villalobos et al., 2003; Wong, 2009; Zeiner et al., 2021). Reductive activation of dioxygen [O2] and production of superoxides/peroxides through metalloenzymes is a common degradation process of detrital organic matter and production of metal-oxo species where available Fe and Mn can play significant roles because of their bioavailability, multiple oxidation states, and coordination complexes (Guo et al., 2019; Olivo et al., 2017; Sahu and Goldberg, 2016). Such enzymatic activity and metal-complex formation can create variable bonding environments (Du et al., 2018; Guo et al., 2019; Olivo et al., 2017). The role of Fe and Mn in such processes can be intertwined (e.g., Fe oxidation by Mn oxides (Bryce et al., 2018)) and can produce differences in oxidation states, complexation, and solubility (Chowdhary et al., 2018; Engelmann et al., 2016; Sawant et al., 2010), which can be primary influences on the release and transport of metals from contaminated sediments into porewater and overlying waters (Kappler et al., 2021; Singh et al., 1984; Wojtkowska, 2013).

Chapter 2: Study area, materials, and methods

The Coeur d'Alene River Basin is located in the Coeur d'Alene Mountains of the Bitterroot Range. The quartzite and argillite containing the ore in the Coeur d'Alene Mining District have been mined since the 1880s and are part of the Mesoproterozoic Belt Supergroup composing the Coeur d'Alene Mountains (Leach et al., 1988). The ore primarily consists of argentiferous galena [PbS] and sphalerite [(Zn,Fe)S] with associated carbonate zones consisting primarily of siderite [FeCO3] and ankerite [Ca(Fe,Mg,Mn)(CO_3)2] (Balistrieri et al., 2003; Balistrieri and Blank, 2008; National Research Council, 2005). An estimated 56 Mt of processed tailings with 900,000 t of Pb and 700,000 t of Zn have been released into the basin floodplains along with unknown amounts of As, Cd, Cu, Fe, Hg, Mn, and Sb (Long, 1998). In addition to the processed tailings, waste rock containing an unknown amount of metal(loid)s was dumped in creek channels/floodplains as a legacy practice of waste disposal. The discarded tailings and waste rock were transported downstream by high streamflows, which distributed it throughout the river floodplain and into Coeur d'Alene Lake (Balistrieri and Blank, 2008; Clark and Mebane, 2014; Langman et al., 2018; National Research Council, 2005). The lake continues to see fluctuations of metal concentrations in the water column, partially from continued loading of metals from the Coeur d'Alene River (Clark and Mebane, 2014) and partially from release of metals from lake sediments during seasonal shifts in environmental conditions (Wood and Beckwith, 2008). Currently, the lake does not experience substantive algal blooms, but lakebed sediments do contain organic matter concentrations of approximately 3–5% (Langman et al., 2020a)

2.1 *Study design*

This study is part of a series of analyses derived from laboratory experiments designed for examination of the potential release of metals under current (anoxic) and possible future (anoxic + additional algal detritus (anoxic + algae)) conditions. The study was designed to replicate SWI conditions during the seasonal shift to anoxic conditions (control group) and a hypothetical condition of anoxia + algae (treatment group) to replicate potential future conditions that include substantive algal blooms and the addition of greater organic matter (algal detritus) to the lakebed. In November 2017, sediment cores were collected from Aberdeen Lodge Bay (Fig. 1, depth ≈ 15 m) in Coeur d'Alene Lake opposite the confluence of the Coeur d'Alene River. This sampling period was selected

because the fall period represents the time of turnover and reoxygenation of the water column and upper sediments (outside of the perceived seasonal hypoxic/anoxic period that forms during summer).

2.2 *Sediment core collection*

The sediment cores were collected in disinfected (70% EtOH, 30% ultrapure water), polyvinyl chloride, core barrels (5.2-cm ID × 61-cm L) that were kept for 48 hr in a positive N2 atmosphere prior to sampling. Using a Kajak-Brinkhurst gravity corer, the core barrels were allowed to free fall from 1 m below the lake surface for collection of sediment samples of 45–50 cm in depth. Head water in the core barrel was siphoned from each sample to minimize disturbance of the sediments during transport. After siphoning, cores were capped, flushed with N2, and stored upright in an N2 atmosphere in gas-tight containers for transport to the University of Idaho Lake Social Ecological Systems (LaSES) Laboratory in Coeur d'Alene, Idaho. At the time of the core collection, lake water was collected 1 m above the SWI using a disinfected, 2-L, Van Dorn sampler. Upon arrival at the LaSES Laboratory, core containers were checked for positive pressure and stored in the dark at 4.5 ˚C under an N2 atmosphere.

2.3 *Algae collection and column loading*

Algae was collected from Fernan Lake (Fig. 1), an adjoining eutrophic lake, by pumping water through 80-µm mesh net followed by centrifugation (3,750 RCF for 15 min), solidification at -20 ºC, lyophilization (Labconco FreeZone freeze dryer), and homogenization by the roll method (Ingamells and Pitard, 1986; Johnson and Maxwell, 1981; Schüler, 1971). To simulate the addition of algal detritus to the lakebed, 0.25 g of the homogenized algae were added to half of the cores along with 325 mL of Coeur d'Alene Lake water to all cores (half of the cores were in the control group and the other half in the treatment group). The amount of algal detritus added to the cores was based on previous sediment analyses of mesotrophic and eutrophic lakes in the Pacific Northwest, USA (Child et al., 2018; Welch, 2009). After input of the lake water or algae + lake water, the cores were capped, flushed with N2, stored at 4.5 ˚C upright in the dark, and under an N2 atmosphere to begin the 8-week experimental period (Langman et al., 2020a).

2.4 *Column experiment*

Cores collected for this experiment were kept in the same anaerobic conditions (N2 atmosphere) from which one control (anoxia) and treatment (anoxia + algae) core were removed and analyzed every two weeks. The cores were deconstructed for collection of sediment samples from 1-cm thick layers centered at 2.5 cm and 12.5 cm below the SWI. These sediments were collected for

X-ray absorption spectroscopy (XAS) to examine Fe and Mn oxidation state distribution and bonding environment and were the same cores and samples examined as part of Langman et al.'s (2020a) evaluation of S oxidation states and bonding environments (XAS cores). For preparation of the sediment samples collected from the XAS cores, porewater was separated from the the 2.5-cm and 12.5-cm sediment samples by centrifugation (3,750 RCF for 15 min) and analyzed for pH, redox potential (ORP), Fe^{2+} by ferrozine method and a ThermoFisher Genesys spectrophotometer, and Fe and Mn concentration by inductively coupled plasma mass spectrometry at the University of Idaho Analytical Sciences Laboratory (ASL). Centrifuged sediments were immediately frozen and dehydrated (lyophilized for 24 h) and preserved at –80 °C. The 2.5-cm sample location represents the near SWI environment where redox-sensitive elements have concentrated (Morra et al., 2015), and the 12.5-cm sample location represents a possible restricted zone because of the low permeability in these silt/clay dominated sediments. This deeper zone was selected for analysis to compare depth penetration of environmental changes that could influence Fe and Mn oxidation state and bonding environment. Deeper sample locations were not considered because of the presence of a volcanic ash layer (Mount St. Helens in 1980) about 15 cm below the SWI that restricts permeability and acts as a metal sorbing substrate (Heap et al., 2018; Jensen et al., 2018).

2.5 *X-ray absorption spectroscopy*

The goal of this study was the temporal evaluation of any shifts in sediment Fe and Mn oxidation states and bonding environments with onset of anoxic conditions and presence of additional algal detritus at the SWI. Synchrotron-based XAS was performed for discriminating Fe and Mn oxidation states and bonding environments at the selected 2.5-cm (upper) and 12.5- cm (lower) sediment depths. A pre-experiment core was sampled at the midpoint of 5-cm intervals (2.5, 7.5, 12.5, etc.) for analysis of element composition with depth to determine metal concentration from the SWI to the bottom of the cores. These sediments were analyzed for element composition by X-ray fluorescence (XRF) at the Washington State University GeoAnalytical Laboratory using an Advant'XP+ sequential XRF spectrometer and construction of fused beads from 5 g of each sediment sample. Synchrotron XAS of the upper and lower sediment samples was performed at the Canadian Light Source, 06B1-1 beamline (SXRMB), in Saskatchewan, Canada. A Si(111) monochromator at 06B1-1 can produce an incident beam energy of 1.7–10 keV. For this study, a 3 × 2 mm beam was used to collect fluorescence mode spectra for X-ray absorption near edge structure (XANES) and extended X-ray absorption fine structure (EXAFS) analysis. The spectra were processed with the XAS program ATHENA (Ravel and Newville, 2005). K-edge energies for the reference materials were determined as the maxima of the first derivative and were shifted to the theoretical values to

account for beamline flux. Each environmental sample was scanned twice to determine if additional scans were needed to reduce the signal-to-noise ratio (minimization of standard deviation near the K-edge). The environmental spectra were calibrated to the energy shift apparent from the applicable reference material, and the spectrum was edge-step normalized (within a maximum 15–80 eV normalization range) for comparison of environmental samples and reference materials. An element's oxidation state distribution can be interpreted from the XANES region of the spectra (Alp et al., 1990; Newville, 2014). Oxidation state distribution of Fe and Mn were determined with ATHENA's linear combination fitting (LCF) capability (Ravel and Newville, 2005) within a K-edge range of –20 eV to +30 eV. The goal of the LCF analysis was to discriminate the oxidation state distributions of Fe and Mn over the experimental period by fitting common Fe and Mn oxidation states from reference materials. LCF was used to reconstruct each sample spectrum using reference material spectra of pyrite [$Fe^{2+}S2$] and goethite [$Fe^{3+}O(OH)$] for Fe and rhodochrosite [$Mn^{2+}CO3$], Mn oxide [Mn^{3+} 2O3], and ramsdellite [$Mn^{4+}O2$] for Mn. Sediment Mn forms did not exhibit a detectable oxidation state lower than Mn^{2+} or higher than Mn^{4+} . An element's coordination number, bond length, and/or local disorder of adjacent atoms can be evaluated through interpretation of the EXAFS region (Sham, 2008), which is a reflection of ejected photoelectrons interacting with the electons of surrounding atoms (scatterers) or what is described as the bonding environment (Alp et al., 1990; Gaur and Shrivastava, 2015; Penner- Hahn, 2005). The EXAFS region of the environmental sample spectra was analyzed for relative shifts in adjacent atom characteristics (e.g., bond length) through changes in 1st and 2nd sphere spectra in frequency filtered (Fourier transformation with k-weight = 2 and Hanning window (or cosine-squared taper)) for R space—magnitude ($\chi(R)$) and real number portion ($Re[\chi(R)]$). The resulting complex number of the transformed spectra (Fourier transformed $\chi(R)$ in Å) has real and imaginary numbers that complete the complex number, which is a reflection of the magnitude of the shell and bonding environment response (e.g., scatter number and disorder) to the electron wavefunction (Koningsberger et al., 2000; Koningsberger and Ramaker, 2008; Newville, 2014). Well differentiated peaks in $\chi(R)$ can indicate primary shells in the bonding environment, although the alteration of $\chi(k)$ to $\chi(R)$ shifts interpreted bond lengths approximately 0.2–0.5 Å (Newville, 2014). Given the number of possible Fe and Mn bonds and more than one type of neighboring atom, changes in lake sediment bonding environments were viewed as relative differences between conditions and with time. Shifts in the bonding environment are reflected in magnitude responses (EXAFS region = summed response of all bonds) and relative radial distances (van Bokhoven et al., 2005), such as differences in typical Fe bond lengths: 1.8 Å for Fe–C (Braga et al., 1993; Chen et al., 2020; Hanson, 1962), 2.1 Å for Fe–O (Hicks et al., 2014), 2.3 Å for Fe–S (Sayers et al., 1976), and 2.5 to 3.1 Å for Fe–Fe (Newville, 2014; Pauling, 1976). Mn–O bonds can be

relatively inflexible with bond lengths between 1.7 and 2.2 Å (Gilbert et al., 2003; Leto and Jackson, 2014). Mn–O bonds are shorter compared to Mn–C bonds, although Mn–O bonds will lengthen with lower Mn oxidation states (Gilbert et al., 2003; Leto and Jackson, 2014). Only the upper sediments samples were examined for bonding environment shifts because of limited changes in the lower sediment oxidation state distributions under both experimental conditions.

Chapter 3: Results

3.1 *Reactive upper sediment layer*

Past studies of Coeur d'Alene Lake found significant concentrations of Ag, As, Cd, Cu, Fe, Hg, Mn, Pb, Sb and Zn in the lakebed sediments (Horowitz et al., 1995a, 1995b). Results of the XRF analysis of the pre-experiment core indicated substantial mining-related metal concentrations and a variation in the distribution of metal concentrations above and below the volcanic ash layer (Fig. 2). The discharge of sediments to the lake following emplacement of the ash layer continued to deposit large concentrations of mining-related elements such as Pb and Zn on the lakebed (Fig. 2). The presence of Fe and Mn in the mined ore body has resulted in the substantial presence of these elements in lake sediments, such as the approximate 10 wt. % as FeO and 1–2 wt. % as MnO in the upper 10 cm (Fig. 2). Results of the XRF analysis for samples from the 45–50 cm interval (below substantial Pb and Zn concentrations) suggests that background concentrations of Fe and Mn as their oxide form may be near 7.5 wt. % and 0.25 wt. %, respectively. The substantial decrease in concentrations of mining-related elements below 40 cm aligns with Harrington et al. (1998a) who indicated a similar decrease in suspected mining impacts below this depth.

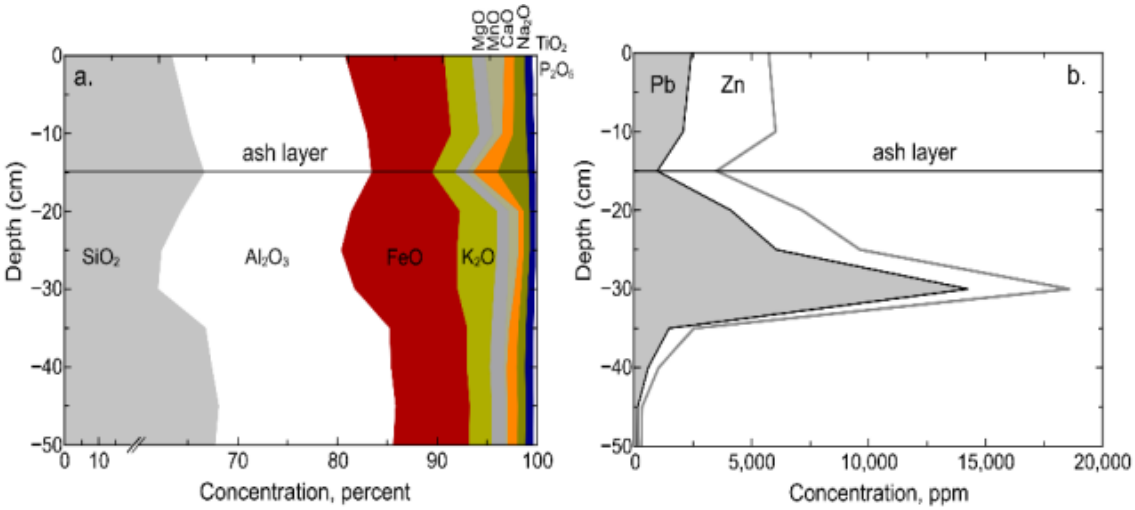

.

Fig. 2. Cumulative area graphs of major (a) and trace element (b) concentrations for sediments collected from Aberdeen Lodge Bay in Coeur d'Alene Lake. Major elements are normalized to 100 percent. Trace element concentrations are not normalized (Langman et al., 2020a).

Langman et al. (2020a) indicated a substantial change in S oxidation states and the release of Mn into porewater during week 2 in the anoxic + algae condition that was not present during the anoxic condition (Fig. 3). The anoxic and anoxic + algae conditions produced dissimilar trends in

porewater Mn concentrations collected from the XAS cores but similar trends in Fe concentrations for upper sediment and similar trends in the lower sediments for Fe and Mn (Fig. 3). The Fe released into porewater in the upper sediments was primarily Fe^{2+}, which ranged from 75 % to 100 % of the Fe detected in the porewater extracted from the sediments collected from the XAS cores. The anoxic + algae condition produced the greatest difference (+12,000 µg/L) in Mn concentrations in the upper

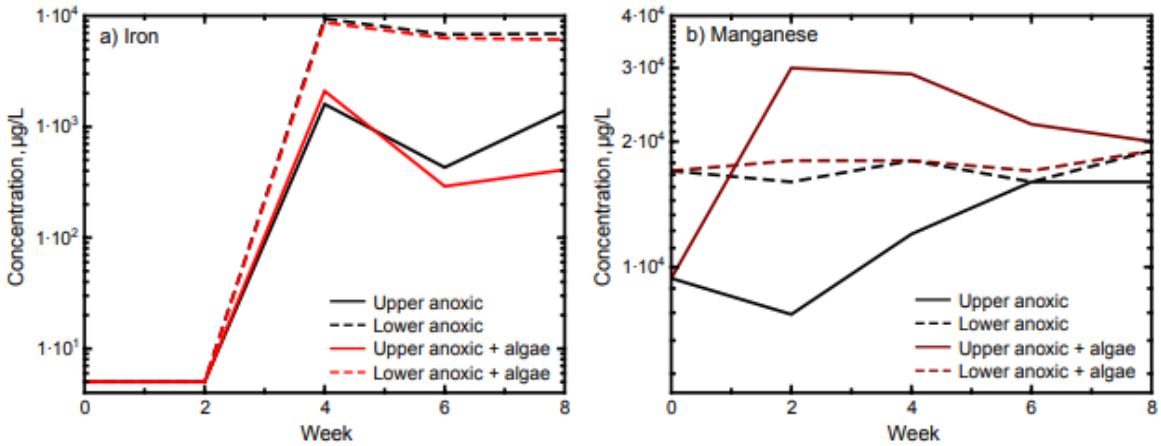

sediments during week 2, although both conditions produced relatively similar porewater Mn concentrations by the end of the experiments.

Fig. 3. Iron and manganese concentrations in porewater extracted from the control (anoxia) and treatment (anoxia + algae) sediment cores over the course of the 8-week experiment (adapted from Langman et al. (2020a)). The upper and lower iron and manganese concentrations are from analysis of the porewater extracted from the corresponding sediment samples collected for X-ray absorption spectroscopy.

3.2 *Iron and manganese oxidation state distribution*

Examination of upper and lower sediment Fe oxidation states (Fig. 4) from the XANES portion of the sediment XAS spectra indicated little change in Fe oxidation state distribution (dominance of Fe^{3+}) under anoxic and anoxic + algae conditions. Both the anoxic and anoxic + algae conditions produced favorable environments for the oxidation of Fe with relatively small amounts of Fe^{2+} (5 % to 25 %) in weeks 2, 6, and 8 (Fig. 4). Results from week 2 indicated the greatest presence of Fe^{2+} in the deeper sediments under both conditions and under the anoxic + algae condition in the upper sediments. The substantial release of Mn into porewater during week 2 in the upper sediments under the anoxic + algae condition (Fig. 3) corresponds to the only detectable presence of Fe^{2+} in the upper sediments (Fig. 4). Upper sediment porewater was neutral (pH range of 6.9 to 7.4) under both conditions throughout the experiment, and ORP varied (range of –83 to 180 mV) but trended from oxidizing to reducing over the 8-week period. The greater presence of detectable Fe^{2+} in the deeper sediments under both conditions occurred under neutral (pH range of 6.7 to 7.4) and reducing (ORP range from –103 to –30 mV) conditions but did not have a substantial effect on the release of Mn into

the porewater of these lower sediments (Fig. 3).

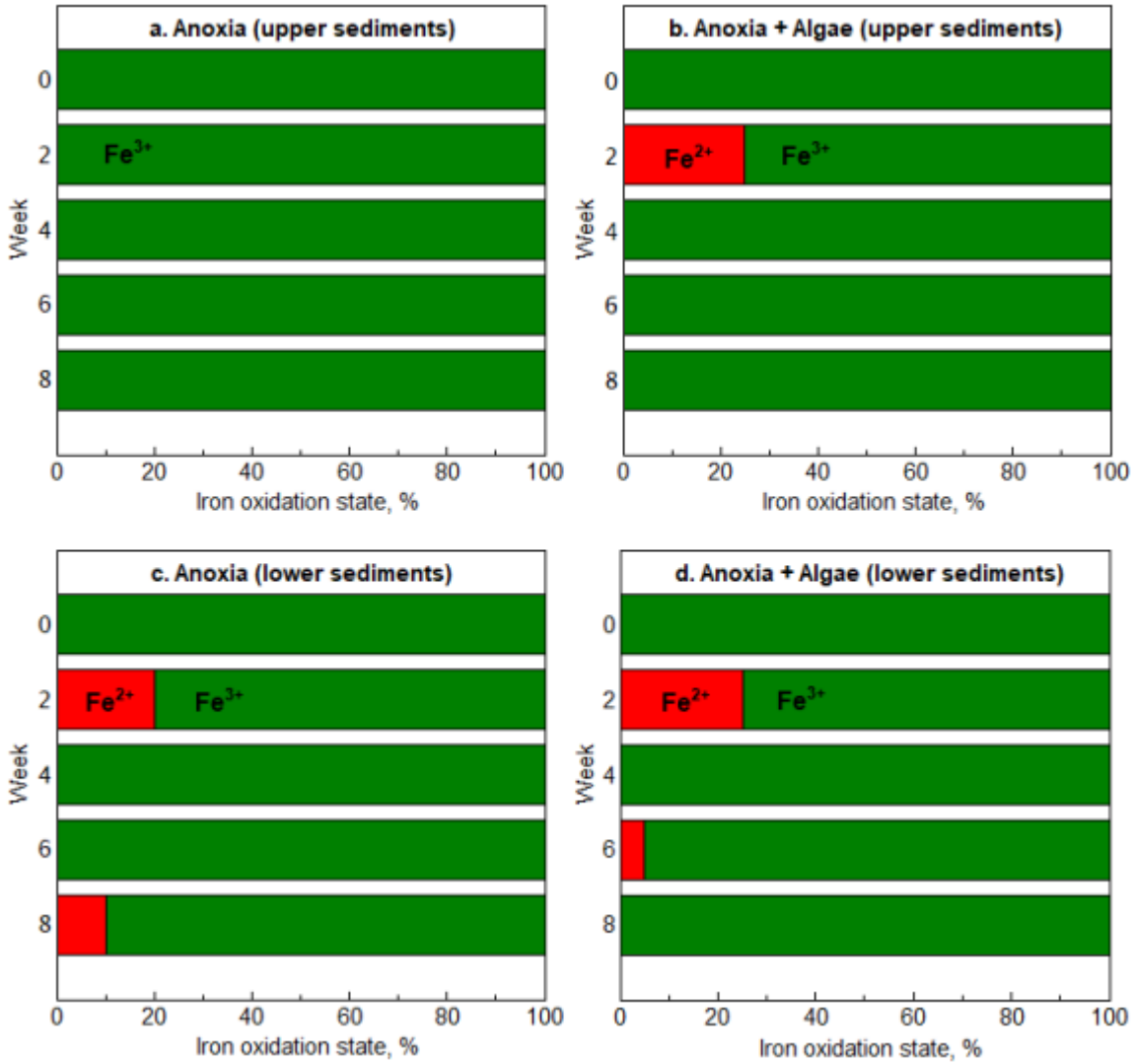

Fig. 4. Distribution of iron oxidation states in upper and lower sediment samples of the control (anoxia) and treatment (anoxia + algae) cores over the course of the 8-week experiment.

The XANES portion of the XAS spectra for Mn in the lower sediments indicated relatively similar patterns of $Mn^{2+/3+}$ oxidation states under the two conditions, except for a divergence in the oxidation state distribution during week 2 (Fig. 5). It appears that the influence of anoxic and anoxic + algae conditions did not have a substantial effect on Mn oxidation state in the deeper sediments and produced primarily reduced Mn (Fig. 5) compared to the dominance of oxidized Fe in these sediments (Fig. 4). The substantial presence of Mn^{3+} in the lower and upper sediments is suggestive of Mn-organo complexes that are able to stabilize Mn in the higher oxidation state under anoxic conditions (Chowdhary et al., 2018; Zeiner et al., 2021). The addition of algae to the upper sediments had a strong influence on Mn oxidation states when compared to the anoxic condition (Fig. 5). With

the addition of algae, oxidation of Mn in the upper sediments progressed during the experiment and produced greater Mn^{3+} and the presence of Mn^{4+} that was not identified with the anoxic condition (Fig. 5).

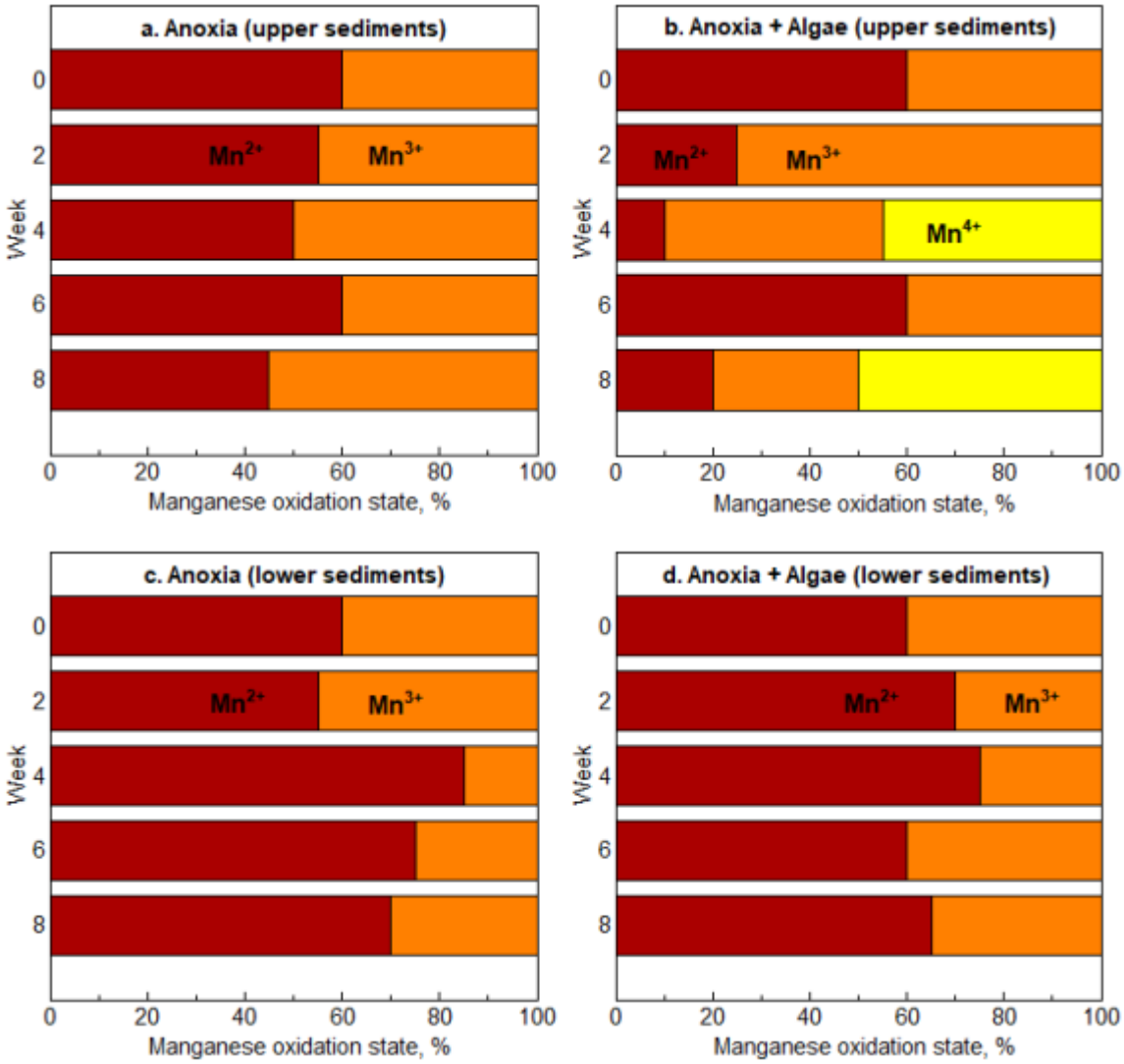

Fig. 5. Distribution of manganese oxidation states in upper and lower sediment samples of the control (anoxia) and treatment (anoxia + algae) cores over the course of the 8-week experiment

3.3 *Upper sediment iron and manganese bond environment*

The Fe EXAFS spectra for the anoxic conditions did not indicate substantial bond shifts during the experiment except for an initial change from the pre-experiment condition (Fig. 6). The pre-experiment condition (Fig. 6) likely represents a mixed state system following holomixis or mixing of the previously stratified layers that re-oxygenated the bottom waters, which shifted the sediment porewater environment from it hypoxic/anoxic condition to a more oxygenated

environment. This change in porewater environment likely initiated multiple redox changes that resulted in Fe forms with multiple scattering paths (broad, low magnitude peaks) that dampened the backscatter response (EXAFS region is a sum of the backscattered waves (Mastelaro and Zanotto, 2018)). With the start of the experiment and persistent anoxic conditions, Fe bonds stabilized at relatively short bond lengths (e.g., Fe–O and/or Fe–C bonds) and remained relatively similar throughout the experiment period under the anoxic and anoxic + algae conditions (Fig. 6). The anoxic + algae condition produced a slight shift in Fe bonds in week 2, but the bonding environment remained relatively stable over the experiment period (Fig. 6b,d). This slight shift in the Fe bonding environment during week 2 corresponds to the increase in Fe^{2+} (Fig. 4) with the anoxic + algae condition. The shift consisted of an earlier 1st sphere magnitude response ($\chi(R)$) suggestive of bond shortening and loss of coordinated structure given the lower magnitude (Fig. 6b). This shift in Fe bonds is reflected in the shorter period in the oscillation of the week 2 real portion ($Re[\chi(R)]$) of the transformed spectra (Fig. 6d) indicative of differences in near-neighbor coordination shells (Newville, 2014).

The bonding environment for Mn under the anoxic condition indicated a shift towards longer bond lengths except during week 6 (Fig. 7a,c). The overall shift towards longer Mn bond lengths under anoxic conditions (Fig. 7c) produced a week 8 dampening effect in the wave backscatter that reduced the period and amplitude of the oscillations (Fig. 7d). With the addition of algae to the SWI, the EXAFS spectra indicated substantial variation in the Mn bonding environnent, such as the longer bond lengths during week 2 and the shorter bond lengths during weeks 4 and 8 (Fig. 7b,d). Under this variable bonding environment, the backscatter oscillations indicated substantial shifts in period and amplitude (Fig. 7d) that reflect the shift in Mn oxidation states (Fig. 5). The relatively short bond lengths in week 4 and 8 correspond with the detection of Mn^{4+} (Fig. 5), which suggests shortened oxide bonds. The likely shifting of bond lengths and ligands (near-neighbor coordination spheres) suggests a cyclic process that fluxed with inputs from the degrading algae (Bryce et al., 2018; Guo et al., 2019; Sahu and Goldberg, 2016).

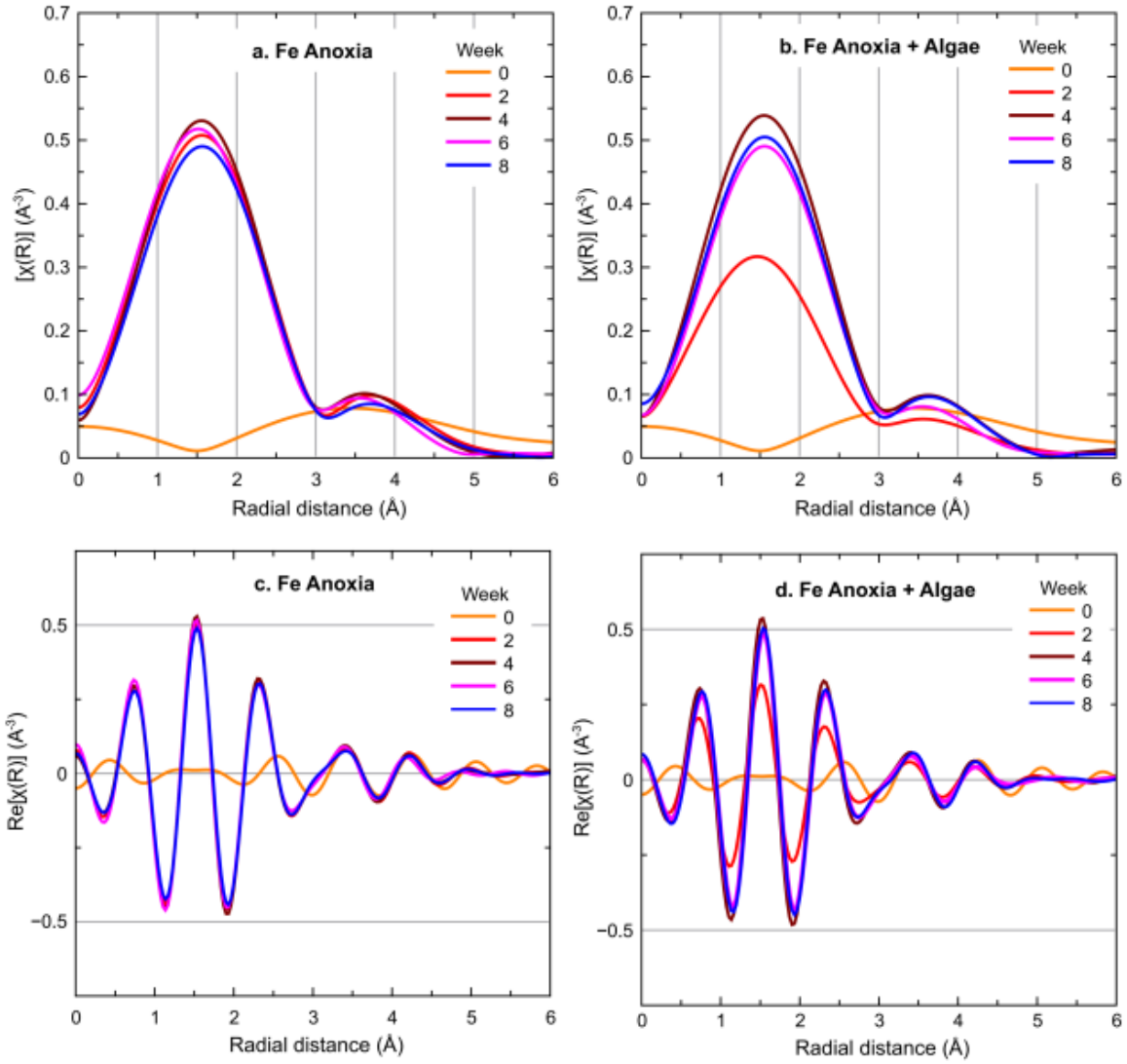

Fig. 6. Fourier transformation of iron EXAFS spectra (magnitude (χ(R)) and real portion (Re[(χ(R)])) for upper sediments from the anoxia and anoxia + algae cores over the course of the 8-week experiment.

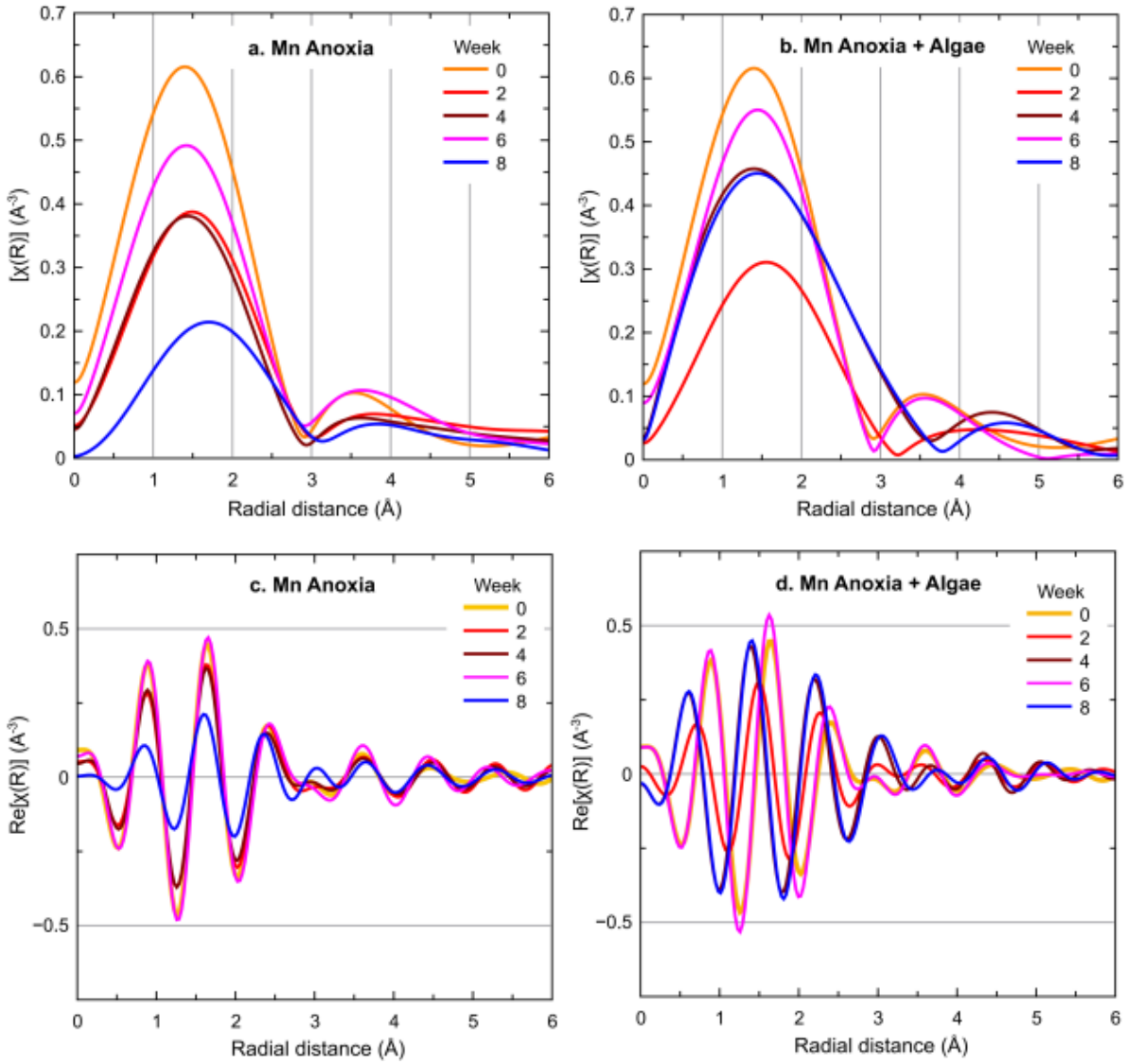

Fig. 7. Fourier transformation of manganese EXAFS spectra (magnitude (χ(R) and real portion Re[(χ(R)])) for upper sediments from the anoxia and anoxia + algae cores over the course of the 8-week experiment

Chapter 4: Discussion

Fe and Mn have intertwined redox chemistries and both metals have soluble reduced forms and generally insoluble (oxyhydr)oxides that will readily shift oxidation states with changes in redox conditions (Davison, 1993). The difference in the $Mn^{3+/}Mn^{2+}$ half reaction (E° = +1.50 V) and the $Fe^{3+/}Fe^{2+}$ half reaction (E° = +0.67 V) can discriminate their roles in biogeochemical cycling because of the greater energy to be derived from Mn redox reactions, although redox potentials will vary with pH and temperature (Bucheli-Witschel and Egli, 2001; LaRowe et al., 2021; Straub et al., 2001). The anoxic + algae conditions were expected to provide additional carbon and nitrogen for stimulation of microbial populations that could produce dissimilatory metal reduction with algae oxidation (Bradley et al., 2011; Plugge et al., 2011), which would correspond to the previous identification of primarily reduced S in the deeper sediments (both conditions) and an increasing trend in reduced S under upper sediment anoxia and variable S oxidation states with the addition of the algae (Langman et al., 2020a). Instead of acting as an electron acceptor, the microbial community assimilated or used sediment-bound Fe as an electron shuttle (e.g., extracellular electron transfer (He et al., 2017)) and also formed organo-Mn complexes by enzymatic processes where Mn can be relatively stable in the Mn^{3+} oxidation state (Fig. 8) (Hofrichter, 2002; Quintanar et al., 2007; Wariishi et al., 1992). Given the general insolubility of Fe^{3+} (oxyhdr)oxides (Baumgartner and Faivre, 2015) and neutral pH of the porewater throughout the experiment, the Fe likely were sediment-bound oxides or held in extracellular locations (cell outer surface or periplasm with Fe^{2+} pump out) that avoid intracellular Fe precipitation and Fe^{2+} toxicity (Bennett and Gralnick, 2019; He et al., 2017; Schädler et al., 2009). These sediment-bound, extracellular locations may be why Fe^{3+} was predominantly identified in the sediment samples (Fig. 4) along with the release of primarily Fe^{2+} to porewater. The Fe^{4+} oxidation state of the example enzymatic process (Fig. 8) was not analyzed in this experiment since Fe^{4+} exists only temporarily as an electron shuttle and the Fe is stabilized as Fe^{3+} (Sundaramoorthy et al., 1994). Given the presence of small concentrations of Fe^{3+} in porewater (0 % to 25 %), Fe^{3+} chelates (Nevin and Lovley, 2002) may have formed and been released into solution as part of such enzymatic processes.

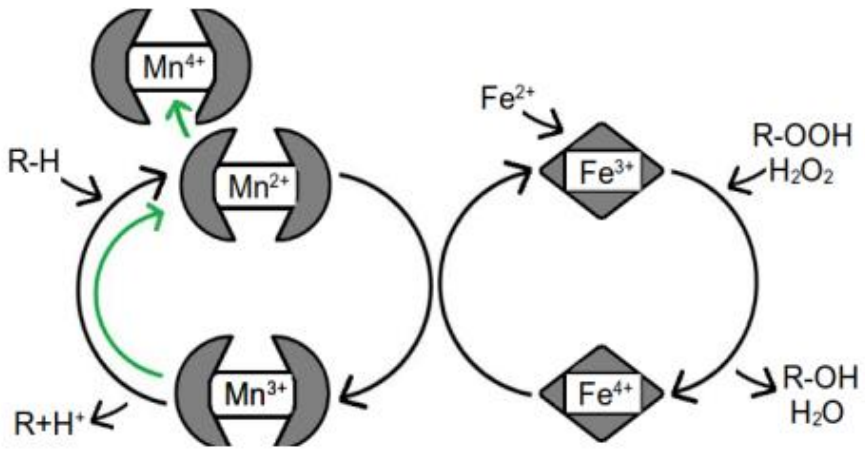

Fig. 8. Schematic of possible enzymatic manganese cycling in the presence of detrital organic matter. The green arrow represents a potential pathway that occurs by means of an oxidase that forms mobile Mn^{4+} (adapted from Hofrichter (2002).

Organo-complexed Mn can be formed by enzymatic activity where oxidized Fe is used as an electron shuttle to oxidize Mn^{2+} with production of $Mn^{3+,4+}$ and Mn-oxalate/lactate chelates (Fig. 8) (Hofrichter, 2002; Kumar and Chandra, 2020). Such processes keep Fe oxidized (Fe^{3+}) while oxidizing Mn and producing various Mn chelates (Abdel-Hamid et al., 2013). The strong prevalence of Mn^{3+}, occasional presence of Mn^{4+} (Fig. 5), variation in the bonding environment of Mn in the anoxic + algae condition (Fig. 7), and large release of Mn into porewater early in the experiment (Fig. 3) indicates the early formation of water-soluble, multidentate Mn chelates (e.g., aminopolycarboxylic acids (Bucheli-Witschel and Egli, 2001)) along with sediment-bound, enzyme-incorporated $Mn^{3+,4+}$ (Soldatova et al., 2017). Oxidoreductase enzymes, such as Mn peroxidase, are present in almost all known bacteria and fungi (Chowdhary et al., 2018) and can provide the mechanism for organic matter degradation and Mn oxidation and mobility (Kumar and Chandra, 2020; Quintanar et al., 2007). With microbially-facilitated Mn^{2+} oxidation, $Mn^{3+/4+}$ can be stabilized through bonding with carboxylic acids, which form compounds that can further oxidize degrading organic matter (Hofrichter, 2002; Kumar and Chandra, 2020; Wong, 2009). Such microbially-facilitated activity likely produced the presence of primarily oxidized Fe in the sediments (Fig. 4) and relatively stable Fe bonding environment (Fig. 6) in both conditions because of the existing presence of available organic matter and microbial population without additional algal detritus. The stability of Fe under anoxic and anoxic + algae conditions is in contrast to the increased oxidation of Mn (Fig. 5) and variable bonding environment with the addition of algae (Fig. 7). This greater variability in Mn oxidation states and bonding environments indicates enhanced enzymatic oxidation and stabilization of higher Mn oxidation states with the greater availability of organic matter (Liu et al., 2020;

Soldatova et al., 2017). Such an enhancement to Mn-involved enzymatic processes (Fig. 8), even under anoxic conditions, likely is responsible for the increased Mn oxidation (Fig. 5), limited change in Fe oxidation (Fig. 4), variable Mn bond lengths (Fig. 7), and release of Mn into porewater under the anoxic + algae conditions in the upper sediments (Fig. 3).

Chapter 5: Conclusion

Legacy mining practices allowed the hydrologic transport of tailings and waste rock from the Coeur d'Alene Mining District to Coeur d'Alene Lake where an estimated 75 Mt of metal(loid)-contaminated sediments have entered the lake over the past 100+ years. Prior studies have indicated that the mining-contaminated sediments of Coeur d'Alene Lake undergo a seasonal anoxia period, which likely will evolve towards a seasonal period of anoxia plus additional algal detritus because of predicted algal blooms. Eight-week, benchtop experiments were conducted for replication of anoxic and anoxic + algae conditions for sediment cores collected from the lakebed. Examination of synchrotron X-ray absorption spectra for Fe and Mn in cored sediments indicated that anoxic conditions produced a relatively stable Fe oxidation state distribution and an increase in Mn oxidation over the experimental period. Correspondingly, the bonding environment of Fe did not significantly change over the course of the experiment, but the Mn bonding environment indicated substantial variation with the addition of the algae. This difference in oxidation state distribution and bonding environment between Fe and Mn likely is a result of the incorporation of Fe as an electron shuttle in an enzymatic process that produces $Mn^{3+/4+}$ organo-complexes. This enzymatic process likely was enhanced with additional organic matter through introduction of the additional algae, which increased Mn oxidation and created a variable bonding environment. As part of this process, Fe is captured or retained at a higher oxidation state in the sediments under anoxic conditions while Mn increases in oxidation and can be released as soluble $Mn^{3+,4+}$ chelates that likely explains the increase of porewater Mn concentrations with the addition of the algae.

References

Abdel-Hamid, A.M., Solbiati, J.O., Cann, I.K.O., 2013. Chapter One - Insights into Lignin Degradation and its Potential Industrial Applications, in: Sariaslani, S., Gadd, G.M. (Eds.), Advances in Applied Microbiology. Academic Press, pp. 1–28. https://doi.org/10.1016/B978-0-12-407679-2.00001-6

Aiken, G.R., Hsu-Kim, H., Ryan, J.N., 2011. Influence of dissolved organic matter on the environmental fate of metals, nanoparticles, and colloids. Environ. Sci. Technol. 45, 3196–3201. https://doi.org/10.1021/es103992s

Alp, E.E., Mini, S.M., Ramanathan, M., 1990. X-ray absorption spectroscopy: EXAFS and XANES - A versatile tool to study the atomic and electronic structure of materials (Workshop report No. ANL/APS/TM--7). Department of Energy, Argonne National Laboratory.

Andeer, P.F., Learman, D.R., McIlvin, M., Dunn, J.A., Hansel, C.M., 2015. Extracellular haem peroxidases mediate Mn(II) oxidation in a marine Roseobacter bacterium via superoxide production. Environ. Microbiol. 17, 3925–3936. https://doi.org/10.1111/1462-2920.12893

Arora, B., Şengör, S.S., Spycher, N.F., Steefel, C.I., 2015. A reactive transport benchmark on heavy metal cycling in lake sediments. Comput. Geosci. 19, 613–633. https://doi.org/10.1007/s10596-0149445-8

Balistrieri, L.S., Blank, R.G., 2008. Dissolved and labile concentrations of Cd, Cu, Pb, and Zn in the South Fork Coeur d'Alene River, Idaho: Comparisons among chemical equilibrium models and implications for biotic ligand models. Appl. Geochem. 23, 3355–3371. https://doi.org/10.1016/j.apgeochem.2008.06.031

Balistrieri, L.S., Bookstrom, A.A., Box, S.E., Ikramuddin, M., 1998. Drainage from adits and tailings piles in the Coeur d'Alene mining district, Idaho; sampling, analytical methods and results (Report No. 98–127), US Geological Survey Open-File Report. U.S. Geological Survey, Reston, VA. https://doi.org/10.3133/ofr98127

Balistrieri, L.S., Box, S.E., Tonkin, J.W., 2003. Modeling precipitation and sorption of elements during mixing of river water and porewater in the Coeur d'Alene River basin. Environ. Sci. Technol. 37, 4694–4701. https://doi.org/10.1021/es0303283

Bargar, J.R., Tebo, B.M., Bergmann, U., Webb, S.M., Glatzel, P., Chiu, V.Q., Villalobos, M., 2005. Biotic and abiotic products of Mn(II) oxidation by spores of the marine Bacillus sp. strain SG-1. Am. Mineral. 90, 143–154. https://doi.org/10.2138/am.2005.1557

Baumgartner, J., Faivre, D., 2015. Iron solubility, colloids and their impact on iron (oxyhydr)oxide formation from solution. Earth-Sci. Rev. 150, 520–530. https://doi.org/10.1016/j.earscirev.2015.09.003

Bennett, B.D., Gralnick, J.A., 2019. Mechanisms of toxicity by and resistance to ferrous iron in anaerobic systems. Free Radic. Biol. Med., Early Life on Earth and Oxidative Stress 140, 167–171. https://doi.org/10.1016/j.freeradbiomed.2019.06.027

Bostick, B.C., Hansel, C.M., Fendorf, S., 2001. Seasonal fluctuations in zinc speciation within a contaminated wetland. Environ. Sci. Technol. 35, 3823–3829. https://doi.org/10.1021/es010549d

Boyle, J., 2001. Redox remobilization and the heavy metal record in lake sediments: a modelling approach. J. Paleolimnol. 26, 423–431. https://doi.org/10.1023/A:1012785525239

Bradley, A.S., Leavitt, W.D., Johnston, D.T., 2011. Revisiting the dissimilatory sulfate reduction pathway.
Geobiology 9, 446–457. https://doi.org/10.1111/j.1472-4669.2011.00292.x

Braga, D., Grepioni, F., Orpen, A.G., 1993. Nickel carbonyl [Ni(CO)4] and iron carbonyl [Fe(CO)5]:
molecular structures in the solid state. Organometallics 12, 1481–1483. https://doi.org/10.1021/om00028a082

Brouwers, G.-J., de Vrind, J.P.M., Corstjens, P.L.A.M., Cornelis, P., Baysse, C., de Vrind-de Jong, E.W., 1999. CumA, a gene encoding a multicopper oxidase, is involved in Mn2+ oxidation in Pseudomonas putida GB-1. Appl. Environ. Microbiol. 65, 1762–1768.
https://doi.org/10.1128/AEM.65.4.1762-1768.1999

Bryce, C., Blackwell, N., Schmidt, C., Otte, J., Huang, Y.-M., Kleindienst, S., Tomaszewski, E., Schad, M., Warter, V., Peng, C., Byrne, J.M., Kappler, A., 2018. Microbial anaerobic Fe(II) oxidation – Ecology, mechanisms and environmental implications. Environ. Microbiol. 20, 3462–3483.
https://doi.org/10.1111/1462-2920.14328

Bucheli-Witschel, M., Egli, T., 2001a. Environmental fate and microbial degradation of aminopolycarboxylic acids. FEMS Microbiol. Rev. 25, 69–106.
https://doi.org/10.1111/j.15746976.2001.tb00572.x

Bucheli-Witschel, M., Egli, T., 2001b. Environmental fate and microbial degradation of aminopolycarboxylic acids. FEMS Microbiol. Rev. 25, 69–106.
https://doi.org/10.1111/j.15746976.2001.tb00572.x

Butterfield, C.N., Soldatova, A.V., Lee, S.-W., Spiro, T.G., Tebo, B.M., 2013. Mn(II,III) oxidation and MnO2 mineralization by an expressed bacterial multicopper oxidase. Proc. Natl. Acad. Sci. 110, 11731–11735. https://doi.org/10.1073/pnas.1303677110

Chen, W.-T., Hsu, C.-W., Lee, J.-F., Pao, C.-W., Hsu, I.-J., 2020. Theoretical Analysis of Fe K-Edge XANES on Iron Pentacarbonyl. ACS Omega 5, 4991–5000.
https://doi.org/10.1021/acsomega.9b03887

Child, A.W., Moore, B.C., Vervoort, J.D., Beutel, M.W., 2018. Bioavailability and uptake of smelter emissions in freshwater zooplankton in northeastern Washington, USA lakes using Pb isotope analysis and trace metal concentrations. Environ. Pollut. 238, 348–358.
https://doi.org/10.1016/j.envpol.2018.03.042

Chowdhary, P., Shukla, G., Raj, G., Ferreira, L.F.R., Bharagava, R.N., 2018. Microbial manganese peroxidase: a ligninolytic enzyme and its ample opportunities in research. SN Appl. Sci. 1, 45. https://doi.org/10.1007/s42452-018-0046-3

Ciszewski, D., Grygar, T.M., 2016. A review of flood-related storage and remobilization of heavy metal pollutants in river systems. Water. Air. Soil Pollut. 227, 239.
https://doi.org/10.1007/s11270-0162934-8

Clark, G., Mebane, C., 2014. Sources, transport, and trends for selected trace metals and nutrients in the Coeur d'Alene and Spokane River basins, Northern Idaho, 1990–2013 (Scientific Investigations Report), Scientific Investigations Report.

Clark, G.M., Mebane, C.A., 2014. Sources, transport, and trends for selected trace metals and nutrients in the Coeur d'Alene and Spokane River Basins, northern Idaho, 1990-2013 (Scientific Investigations Report No. US Geological Survey Scientific Investigations Report 2014-5204). U.S. Geological Survey, Reston, VA.

Cummings, D.E., March, A.W., Bostick, B., Spring, S., Caccavo, F., Fendorf, S., Rosenzweig, R.F., 2000. Evidence for microbial Fe(III) reduction in anoxic, mining-impacted lake

sediments (Lake Coeur d'Alene, Idaho). Appl. Environ. Microbiol. 66, 154–162. https://doi.org/10.1128/AEM.66.1.154162.2000

Davison, W., 1993a. Iron and manganese in lakes. Earth-Sci. Rev. 34, 119–163. https://doi.org/10.1016/0012-8252(93)90029-7

Davison, W., 1993b. Iron and manganese in lakes. Earth-Sci. Rev. 34, 119–163. https://doi.org/10.1016/0012-8252(93)90029-7

Du, J., Miao, C., Xia, C., Lee, Y.-M., Nam, W., Sun, W., 2018. Mechanistic Insights into the Enantioselective Epoxidation of Olefins by Bioinspired Manganese Complexes: Role of Carboxylic Acid and Nature of Active Oxidant. ACS Catal. 8, 4528–4538. https://doi.org/10.1021/acscatal.8b00874

Engelmann, X., Monte-Pérez, I., Ray, K., 2016. Oxidation Reactions with Bioinspired Mononuclear NonHeme Metal–Oxo Complexes. Angew. Chem. Int. Ed. 55, 7632–7649. https://doi.org/10.1002/anie.201600507

Farley, M., 2012. Eutrophication in Fresh Waters: An International Review, in: Bengtsson, L., Herschy, R.W., Fairbridge, R.W. (Eds.), Encyclopedia of Lakes and Reservoirs. Springer Netherlands, Dordrecht, pp. 258–270. https://doi.org/10.1007/978-1-4020-4410-6_79

Gadd, G.M., 2004. Microbial influence on metal mobility and application for bioremediation. Geoderma, Biogeochemical processes and the role of heavy metals in the soil environment 122, 109–119. https://doi.org/10.1016/j.geoderma.2004.01.002

Gao, Y., Kan, A.T., Tomson, M.B., 2003. Critical evaluation of desorption phenomena of heavy metals from natural sediments. Environ. Sci. Technol. 37, 5566–5573. https://doi.org/10.1021/es034392w

Gaur, A., Shrivastava, B.D., 2015. Speciation using X-ray absorption fine structure (XAFS). Rev. J. Chem. 5, 361–398. https://doi.org/10.1134/S2079978015040032

Gilbert, B., Frazer, B.H., Belz, A., Conrad, P.G., Nealson, K.H., Haskel, D., Lang, J.C., Srajer, G., De Stasio, G., 2003. Multiple scattering calculations of bonding and X-ray absorption spectroscopy of manganese oxides. J. Phys. Chem. A 107, 2839–2847. https://doi.org/10.1021/jp021493s

Gozzard, E., Mayes, W.M., Potter, H.A.B., Jarvis, A.P., 2011. Seasonal and spatial variation of diffuse (non-point) source zinc pollution in a historically metal mined river catchment, UK. Environ. Pollut., Nitrogen Deposition, Critical Loads and Biodiversity 159, 3113–3122. https://doi.org/10.1016/j.envpol.2011.02.010

Guo, M., Corona, T., Ray, K., Nam, W., 2019. Heme and Nonheme High-Valent Iron and Manganese Oxo Cores in Biological and Abiological Oxidation Reactions. ACS Cent. Sci. 5, 13–28. https://doi.org/10.1021/acscentsci.8b00698

Hamilton-Taylor, J., Davison, W., Morfett, K., 1996. The biogeochemical cycling of Zn, Cu, Fe, Mn, and dissolved organic C in a seasonally anoxic lake. Limnol. Oceanogr. 41, 408–418. https://doi.org/10.4319/lo.1996.41.3.0408

Hanson, A.W., 1962. The crystal structure of iron pentacarbonyl. Acta Crystallogr. 15, 930–933. https://doi.org/10.1107/S0365110X62003771

Harrington, J.M., Fendorf, S.E., Rosenzweig, R.F., 1998. Biotic generation of arsenic(III) in metal(loid)contaminated freshwater lake sediments. Environ. Sci. Technol. 32, 2425–2430. https://doi.org/10.1021/es971129k

Harrington, J.M., LaForce, M.J., Rember, W.C., Fendorf, S.E., Rosenzweig, R.F., 1998a. Phase associations and mobilization of iron and trace elements in Coeur d'Alene Lake, Idaho. Environ. Sci. Technol. 32, 650–656. https://doi.org/10.1021/es970492o

Haus, K.L., Hooper, R.L., Strumness, L.A., Mahoney, J.B., 2008. Analysis of arsenic speciation in mine contaminated lacustrine sediment using selective sequential extraction, HR-ICPMS and TEM. Appl. Geochem. 23, 692–704. https://doi.org/10.1016/j.apgeochem.2007.11.005

He, S., Barco, R.A., Emerson, D., Roden, E.E., 2017. Comparative genomic analysis of neutrophilic iron(II) oxidizer genomes for candidate genes in extracellular electron transfer. Front. Microbiol. 8.

Heap, M.J., Reuschlé, T., Farquharson, J.I., Baud, P., 2018. Permeability of volcanic rocks to gas and water. J. Volcanol. Geotherm. Res. 354, 29–38. https://doi.org/10.1016/j.jvolgeores.2018.02.002

Hicks, L., Bridges, J., Gurman, S.J., 2014. Ferric saponite and serpentine in the nakhlite Martian meteorites. Geochim. Cosmochim. Acta 136, 194–210. https://doi.org/10.1016/j.gca.2014.04.010

Hoffmann, S.R., Shafer, M.M., Armstrong, D.E., 2007. Strong colloidal and dissolved organic ligands binding copper and zinc in rivers. Environ. Sci. Technol. 41, 6996–7002. https://doi.org/10.1021/es070958v

Hofrichter, M., 2002. Review: Lignin conversion by manganese peroxidase (MnP). Enzyme Microb. Technol. 30, 454–466. https://doi.org/10.1016/S0141-0229(01)00528-2

Horowitz, A.J., Elrick, K.A., Robbins, J.A., Cook, R.B., 1995a. A summary of the effects of mining and related activities on the sediment-trace element geochemistry of Lake Coeur d'Alene, Idaho, USA. J. Geochem. Explor., Heavy Metal Aspects of Mining Pollution and Its Remediation 52, 135–144. https://doi.org/10.1016/0375-6742(94)00041-9

Horowitz, A.J., Elrick, K.A., Robbins, J.A., Cook, R.B., 1995b. Effect of mining and related activities on the sediment trace element geochemistry of Lake Coeur d'Alene, Idaho, USA part II: Subsurface sediments. Hydrol. Process. 9, 35–54. https://doi.org/10.1002/hyp.3360090105

Ingamells, C.O., Pitard, F.F., 1986. Applied Geochemical Analysis, Chemical analysis 88. Wiley, New York.

Jensen, L.C., Becerra, J.R., Escudey, M., 2018. Impact of physical/chemical properties of volcanic ashderived soils on mechanisms involved during sorption of ionisable and non-ionisable herbicides, Advanced Sorption Process Applications. IntechOpen. https://doi.org/10.5772/intechopen.81155 Johnson, W.M., Maxwell, J.A., 1981. Rock and Mineral Analysis, 2nd ed. Wiley & Sons, New York.

Koningsberger, D.C., Mojet, B.L., van Dorssen, G.E., Ramaker, D.E., 2000. XAFS spectroscopy; fundamental principles and data analysis. Top. Catal. 10, 143–155. https://doi.org/10.1023/A:1019105310221

Koningsberger, D.C., Ramaker, D.E., 2008. Applications of X-ray Absorption Spectroscopy in Heterogeneous Catalysis: EXAFS, Atomic XAFS, and Delta XANES, in: Handbook of Heterogeneous Catalysis. American Cancer Society, pp. 774–803. https://doi.org/10.1002/9783527610044.hetcat0040

Kretzschmar, R., Schäfer, T., 2005. Metal retention and transport on colloidal particles in the environment. Elements 1, 205–210. https://doi.org/10.2113/gselements.1.4.205

Kumar, A., Chandra, R., 2020. Ligninolytic enzymes and its mechanisms for degradation of lignocellulosic waste in environment. Heliyon 6. https://doi.org/10.1016/j.heliyon.2020.e03170

Kuwabara, J.S., Topping, B.R., Woods, P.F., Carter, J.L., 2007. Free zinc ion and dissolved orthophosphate effects on phytoplankton from Coeur d'Alene Lake, Idaho. Environ. Sci. Technol. 41, 2811–2817. https://doi.org/10.1021/es062923l

La Force, M.J., Hansel, C.M., Fendorf, S., 2000. Arsenic speciation, seasonal transformations, and Codistribution with iron in a mine waste-influenced palustrine emergent wetland. Environ. Sci. Technol. 34, 3937–3943. https://doi.org/10.1021/es0010150

Langman, J.B., Ali, J.D., Child, A.W., Wilhelm, F.M., Moberly, J.G., 2020a. Sulfur species, bonding environment, and metal mobilization in mining-impacted lake sediments: Column experiments replicating seasonal anoxia and deposition of algal detritus. Minerals 10, 849. https://doi.org/10.3390/min10100849

Langman, J.B., Behrens, D., Moberly, J.G., 2020b. Seasonal formation and stability of dissolved metal particles in mining-impacted, lacustrine sediments. J. Contam. Hydrol. 232, 103655. https://doi.org/10.1016/j.jconhyd.2020.103655

Langman, J.B., Torso, K., Moberly, J.G., 2018. Seasonal and basinal influences on the formation and transport of dissolved trace metal forms in a mining-impacted riverine environment. Hydrology 5, 35. https://doi.org/10.3390/hydrology5030035

LaRowe, D.E., Carlson, H.K., Amend, J.P., 2021. The energetic potential for undiscovered manganese metabolisms in nature. Front. Microbiol. 12. https://doi.org/10.3389/fmicb.2021.636145

Leach, D.L., Landis, G.P., Hofstra, A.H., 1988. Metamorphic origin of the Coeur d'Alene base- and precious-metal veins in the Belt basin, Idaho and Montana. Geology 16, 122–125. https://doi.org/10.1130/0091-7613(1988)016<0122:MOOTCD>2.3.CO;2

Leto, D.F., Jackson, T.A., 2014. Mn K-edge X-ray absorption studies of oxo- and hydroxomanganese(IV) complexes: Experimental and theoretical insights into pre-edge properties. Inorg. Chem. 53, 6179–6194. https://doi.org/10.1021/ic5006902

Liu, W., Hao, J., Elzinga, E.J., Piotrowiak, P., Nanda, V., Yee, N., Falkowski, P.G., 2020. Anoxic photogeochemical oxidation of manganese carbonate yields manganese oxide. Proc. Natl. Acad. Sci. 117, 22698–22704. https://doi.org/10.1073/pnas.2002175117

Long, K.R., 1998. Open-File Report (Open-File Report), Production and disposal of mill tailings in the Coeur D'Alene mining region, Shoshone County, Idaho; preliminary estimates. U.S. Geological Survey, Reston, VA.

Martin, A.J., Pedersen, T.F., 2002. Seasonal and Interannual Mobility of Arsenic in a Lake Impacted by Metal Mining. Environ. Sci. Technol. 36, 1516–1523. https://doi.org/10.1021/es0108537

Mastelaro, V.R., Zanotto, E.D., 2018. X-ray Absorption Fine Structure (XAFS) Studies of Oxide Glasses —A 45-Year Overview. Materials 11, 204. https://doi.org/10.3390/ma11020204

Melton, E.D., Swanner, E.D., Behrens, S., Schmidt, C., Kappler, A., 2014. The interplay of microbially mediated and abiotic reactions in the biogeochemical Fe cycle. Nat. Rev. Microbiol. 12, 797–808. https://doi.org/10.1038/nrmicro3347

Morfett, K., Davison, W., Hamilton-Taylor, J., 1988. Trace metal dynamics in a seasonally anoxic lake. Environ. Geol. Water Sci. 11, 107–114. https://doi.org/10.1007/BF02587769

Morra, M.J., Carter, M.M., Rember, W.C., Kaste, J.M., 2015. Reconstructing the history of mining and remediation in the Coeur d'Alene, Idaho Mining District using lake sediments. Chemosphere 134, 319–327. https://doi.org/10.1016/j.chemosphere.2015.04.055

Murray, K.J., Tebo, B.M., 2007. Cr(III) is indirectly oxidized by the Mn(II)-oxidizing Bacterium Bacillus sp. strain SG-1. Environ. Sci. Technol. 41, 528–533. https://doi.org/10.1021/es0615167

National Research Council, 2005a. Superfund and mining megasites: Lessons from the Coeur d'Alene River Basin (No. ISBN-13: 978-0309097147). The National Academies of Sciences, Engineering, Medicine, Washington, DC.

National Research Council, 2005b. Superfund and Mining Megasites: Lessons from the Coeur d'Alene River Basin. The National Academies Press, Washington, DC. https://doi.org/10.17226/11359

Nealson, K.H., Saffarini, D., 1994. Iron and manganese in anaerobic respiration: Environmental significance, physiology, and regulation. Annu. Rev. Microbiol. 48, 311–343. https://doi.org/10.1146/annurev.mi.48.100194.001523

Nelson, Y.M., Lion, L.W., Ghiorse, W.C., Shuler, M.L., 1999. Production of Biogenic Mn Oxides by Leptothrix discophora SS-1 in a Chemically Defined Growth Medium and Evaluation of Their Pb Adsorption Characteristics. Appl. Environ. Microbiol. 65, 175–180. https://doi.org/10.1128/AEM.65.1.175-180.1999

Nevin, K.P., Lovley, D.R., 2002. Mechanisms for Fe(III) oxide reduction in sedimentary environments. Geomicrobiol. J. 19, 141–159. https://doi.org/10.1080/01490450252864253

Newville, M., 2014. Fundamentals of XAFS. Rev. Mineral. Geochem. 78, 33–74. https://doi.org/10.2138/rmg.2014.78.2

Ni, Z., Wang, S., Wang, Y., 2016. Characteristics of bioavailable organic phosphorus in sediment and its contribution to lake eutrophication in China. Environ. Pollut. 219, 537–544. https://doi.org/10.1016/j.envpol.2016.05.087

Olivo, G., Cussó, O., Borrell, M., Costas, M., 2017. Oxidation of alkane and alkene moieties with biologically inspired nonheme iron catalysts and hydrogen peroxide: from free radicals to stereoselective transformations. JBIC J. Biol. Inorg. Chem. 22, 425–452. https://doi.org/10.1007/s00775-016-1434-z

Palmer, M.J., Chételat, J., Richardson, M., Jamieson, H.E., Galloway, J.M., 2019. Seasonal variation of arsenic and antimony in surface waters of small subarctic lakes impacted by legacy mining pollution near Yellowknife, NT, Canada. Sci. Total Environ. 684, 326–339. https://doi.org/10.1016/j.scitotenv.2019.05.258

Pauling, L., 1976. Metal-metal bond lengths in complexes of transition metals*. Proc. Natl. Acad. Sci. 73, 4290–4293. https://doi.org/10.1073/pnas.73.12.4290

Paulson, A.J., 2001. Biogeochemical removal of Zn and Cd in the Coeur d'Alene River (Idaho, USA), downstream of a mining district. Sci. Total Environ. 278, 31–44. https://doi.org/10.1016/S00489697(00)00886-X

Pedersen, T.F., 1996. A comment on the future environmental status of Coeur d'Alene Lake, Idaho. Northwest Sci. 70, 179–182.

Penner Hahn, J.E., 2005. X-ray absorption spectroscopy. eLS. https://doi.org/10.1038/npg.els.0002984-

Plathe, K.L., von der Kammer, F., Hassellöv, M., Moore, J.N., Murayama, M., Hofmann, T., Hochella, M.F., 2013. The role of nanominerals and mineral nanoparticles in the transport of toxic trace metals: Field-flow fractionation and analytical TEM analyses after nanoparticle isolation and density separation. Geochim. Cosmochim. Acta 102, 213–225. https://doi.org/10.1016/j.gca.2012.10.029

Plugge, C., Zhang, W., Scholten, J., Stams, A., 2011. Metabolic flexibility of sulfate-reducing bacteria. Front. Microbiol. 2.

Qin, X., Sun, X., Huang, H., Bai, Y., Wang, Y., Luo, H., Yao, B., Zhang, X., Su, X., 2017. Oxidation of a non-phenolic lignin model compound by two Irpex lacteus manganese peroxidases: evidence for implication of carboxylate and radicals. Biotechnol. Biofuels 10, 103. https://doi.org/10.1186/s13068-017-0787-z

Quintanar, L., Stoj, C., Taylor, A.B., Hart, P.J., Kosman, D.J., Solomon, E.I., 2007. Shall We Dance? How A Multicopper Oxidase Chooses Its Electron Transfer Partner. Acc. Chem. Res. 40, 445–452. https://doi.org/10.1021/ar600051a

Ravel, B., Newville, M., 2005. ATHENA, ARTEMIS, HEPHAESTUS: data analysis for X-ray absorption spectroscopy using IFEFFIT. J. Synchrotron Radiat. 12, 537–541. https://doi.org/10.1107/S0909049505012719

Sahu, S., Goldberg, D.P., 2016. Activation of Dioxygen by Iron and Manganese Complexes: A Heme and Nonheme Perspective. J. Am. Chem. Soc. 138, 11410–11428. https://doi.org/10.1021/jacs.6b05251

Sarmiento, A.M., Caraballo, M.A., Sanchez-Rodas, D., Nieto, J.M., Parviainen, A., 2012. Dissolved and particulate metals and arsenic species mobility along a stream affected by Acid Mine Drainage in the Iberian Pyrite Belt (SW Spain). Appl. Geochem. 27, 1944–1952. https://doi.org/10.1016/j.apgeochem.2012.07.012

Sawant, S.C., Wu, X., Cho, J., Cho, K.-B., Kim, S.H., Seo, M.S., Lee, Y.-M., Kubo, M., Ogura, T., Shaik, S., Nam, W., 2010. Water as an Oxygen Source: Synthesis, Characterization, and Reactivity
Studies of a Mononuclear Nonheme Manganese(IV) Oxo Complex. Angew. Chem. Int. Ed. 49, 8190–8194. https://doi.org/10.1002/anie.201000819

Sayers, D.E., Stern, E.A., Herriott, J.R., 1976. Measurement of Fe–S bond lengths in rubredoxin using extended x ray absorption fine structure (EXAFS). J. Chem. Phys. 64, 427–428. https://doi.org/10.1063/1.431938

Schädler, S., Burkhardt, C., Hegler, F., Straub, K., Miot, J., Benzerara, K., 2009. Formation of cell-ironmineral aggregates by phototrophic and nitratereducing anaerobic Fe (II)-oxidizing bacteria.
Geomicrobiol. J. 26, 93–103. https://doi.org/10.1080/01490450802660573

Schüler, V.C.O., 1971. Chemical Analysis and Sample Preparation, in: Wainerdi, R.E., Uken, E.A. (Eds.),
Modern Methods of Geochemical Analysis, Monographs in Geoscience. Springer US, Boston, MA, pp. 53–71. https://doi.org/10.1007/978-1-4684-1830-9_3

Schulz-Zunkel, C., Krueger, F., 2009. Trace metal dynamics in floodplain soils of the River Elbe: A review. J. Environ. Qual. 38, 1349–1362. https://doi.org/10.2134/jeq2008.0299

Şengör, S.S., Spycher, N.F., Ginn, T.R., Sani, R.K., Peyton, B., 2007. Biogeochemical reactive–diffusive transport of heavy metals in Lake Coeur d'Alene sediments. Appl. Geochem. 22, 2569–2594. https://doi.org/10.1016/j.apgeochem.2007.06.011

Sham, T. k., 2008. Nanoparticles and nanowires: Synchrotron spectroscopy studies. Int. J. Nanotechnol. 5, 1194–1246. https://doi.org/10.1504/IJNT.2008.019837

Smith, K.S., Huyck, H.L.O., 1999. An overview of the abundance, relative mobility, bioavailability, and human toxicity of metals, in: An Overview of the Abundance, Relative Mobility, Bioavailability, and Human Toxicity of Metals: The Environmental Geochemistry of Mineral Deposits:
Processes, Techniques, and Health Issues. Society of Economic Geologists, Littleton, CO, pp. 29– 70.

Soldatova, A.V., Romano, C.A., Tao, L., Stich, T.A., Casey, W.H., Britt, R.D., Tebo, B.M., Spiro, T.G., 2017. Mn(II) oxidation by the multicopper oxidase complex Mnx: A coordinated two-stage Mn(II)/(III) and Mn(III)/(IV) mechanism. J. Am. Chem. Soc. 139, 11381–11391.
https://doi.org/10.1021/jacs.7b02772

Stone, A.T., Morgan, J.J., 1984. Reduction and dissolution of manganese(III) and manganese(IV) oxides by organics. 1. Reaction with hydroquinone. Environ. Sci. Technol. 18, 450–456.
https://doi.org/10.1021/es00124a011

Sunda, W.G., Kieber, D.J., 1994. Oxidation of humic substances by manganese oxides yields lowmolecular-weight organic substrates. Nature 367, 62–64.
https://doi.org/10.1038/367062a0

Sundaramoorthy, M., Kishi, K., Gold, M.H., Poulos, T.L., 1994. The crystal structure of manganese peroxidase from Phanerochaete chrysosporium at 2.06-A resolution. J. Biol. Chem. 269, 32759– 32767. https://doi.org/10.1016/S0021-9258(20)30056-9

Toevs, G., Morra, M.J., Winowiecki, L., Strawn, D., Polizzotto, M.L., Fendorf, S., 2008. Depositional influences on porewater arsenic in sediments of a mining-contaminated freshwater lake. Environ.
Sci. Technol. 42, 6823–6829. https://doi.org/10.1021/es800937t

Villalobos, M., Toner, B., Bargar, J., Sposito, G., 2003. Characterization of the manganese oxide produced by pseudomonas putida strain MnB1. Geochim. Cosmochim. Acta 67, 2649–2662.
https://doi.org/10.1016/S0016-7037(03)00217-5

Violante, A., Cozzolino, V., Perelomov, L., Caporale, A.G., Pigna, M., 2010. Mobility and bioavailability of heavy metals and metalloids in soil environments. J. Soil Sci. Plant Nutr. 10, 268–292.
https://doi.org/10.4067/S0718-95162010000100005

Wang, F., Liu, C., Liang, X., Wei, Z., 2003. Remobilization of trace metals induced by microbiological activities near sediment-water interface, Aha Lake, Guiyang. Chin. Sci. Bull. 48, 2352–2356. https://doi.org/10.1360/03wd0013

Wariishi, H., Valli, K., Gold, M.H., 1992. Manganese(II) oxidation by manganese peroxidase from the basidiomycete Phanerochaete chrysosporium. Kinetic mechanism and role of chelators. J. Biol.
Chem. 267, 23688–23695. https://doi.org/10.1016/S0021-9258(18)35893-9

Welch, E.B., 2009. Should nitrogen be reduced to manage eutrophication if it is growth limiting?
Evidence from Moses Lake. Lake Reserv. Manag. 25, 401–409.
https://doi.org/10.1080/07438140903323757

Wong, D.W.S., 2009. Structure and action mechanism of ligninolytic enzymes. Appl. Biochem. Biotechnol. 157, 174–209. https://doi.org/10.1007/s12010-008-8279-z

Wood, M.S., Beckwith, M.A., 2008. Coeur d'Alene Lake, Idaho: Insights Gained From Limnological Studies of 1991–92 and 2004–06 (US Geological Survey Scientific Investigations Report No. 2008–5168). U.S. Geological Survey, Reston, VA.

Wood, Molly S., Beckwith, M.A., 2008. Coeur d'Alene Lake, Idaho: Insights gained from limnological studies of 1991-92 and 2004-06 (USGS Numbered Series No. 2008–5168), Coeur d'Alene Lake,
Idaho: Insights Gained From Limnological Studies of 1991-92 and 2004-06, Scientific Investigations Report. Geological Survey (U.S.). https://doi.org/10.3133/sir20085168

Woods, P.F., Beckwith, M.A., 1997. Nutrient and trace-element enrichment of Coeur d'Alene Lake, Idaho (USGS Numbered Series No. 2485), Nutrient and trace-element enrichment of Coeur d'Alene Lake, Idaho, Water Supply Paper. U.S. Geological Survey ; For sale by Information Services,. https://doi.org/10.3133/wsp2485

Zeiner, C.A., Purvine, S.O., Zink, E., Wu, S., Paša-Tolić, L., Chaput, D.L., Santelli, C.M., Hansel, C.M., 2021. Mechanisms of manganese(II) oxidation by filamentous ascomycete fungi vary with species and time as a function of secretome composition. Front. Microbiol. 12.